# Trapping in quantum chains

## J.C. Eilbeck [*], F. Palmero [1]

*Department of Mathematics, Heriot-Watt University, Riccarton, Edinburgh EH14 4AS, UK*

## Abstract

A quantum breather on a translationally invariant one-dimensional anharmonic lattice is an extended Bloch state with two or more particles in a strongly correlated state. In this Letter we study a periodic lattice containing bosons described by the quantum discrete nonlinear Schrödinger equation (QDNLS), a quantum version of the discrete nonlinear Schrödinger equation, also known as the boson Hubbard model. We discuss several effects that break the lattice symmetry and lead to spatial localization of the breather.
© 2004 Elsevier B.V. All rights reserved.

*PACS:* 63.20.Pw; 63.20.Ry; 63.50.+x

*Keywords:* Anharmonic quantum lattices; Quantum breathers; Quantum lattice solitons

## 1. Introduction

The localization of energy by nonlinearity in classical lattices has been much studied recently. Corresponding localized states, called intrinsic localized modes or discrete breathers, have been the subject of intense theoretical and experimental investigation [1]. Results on the quantum equivalent of discrete classical breathers are less numerous, cf. [2,3] for some theoretical results and [4] for some experimental work. Studies of quantum modes on small lattices may be relevant to studies of quantum dots and quantum computing (cf. [5]), and for studies of Bose–Einstein condensates in periodic optical traps [6].

In this Letter, we present some results related to quantum lattice problems, in particular in one-dimensional lattices with a small number of quanta. We study a periodic lattice with $f$ sites containing bosons, described by the quantum discrete nonlinear Schrödinger equation (QDNLS), also known as the boson Hubbard model. This is a quantum version of the discrete nonlinear Schrödinger equation, a particularly simple model for a lattice of coupled anharmonic

---

[*] Corresponding author.
 *E-mail address:* j.c.eilbeck@hw.ac.uk (J.C. Eilbeck).
 [1] Permanent address: Nonlinear Physics Group, Escuela Técnica Superior de Ingeniería Informática, Departamento de Fisica Aplicada I, Universidad de Sevilla, Avda, Reina Mercedes, s/n. 41012 Sevilla, Spain.

oscillators, which has been used to describe the dynamics of a great variety of systems [7]. The QDNLS Hamiltonian is given by

$$\hat{H} = -\sum_{j=1}^{f} \frac{1}{2}\gamma_j b_j^\dagger b_j^\dagger b_j b_j + \epsilon_j b_j^\dagger (b_{j-1} + b_{j+1}), \quad (1)$$

where $b_j^\dagger$ and $b_j$ are standard bosonic operators, $\gamma_j/\epsilon_j$ is the ratio of anharmonicity to nearest neighbor hopping energy, and the chain is subject to periodic boundary conditions with period $f$. Initially we consider the case where the chain is translationally invariant, i.e., $\gamma_j = \gamma$ and $\epsilon_j = \epsilon$ are independent of $j$. In general we take $\epsilon = 1$.

The Hamiltonian (1) has an important conserved quantity, the number $N = \sum_{j=1}^{f} b_j^\dagger b_j$, which enables the total Hamiltonian to be block-diagonalised and greatly simplifies the analysis. In this Letter we restrict ourselves to a study of small lattices and a small number of quanta where numerically exact solutions can be found. Initially we focus on the simplest nontrivial case, $N = 2$, where bound states corresponds to bound two-vibron states, as observed experimentally in several systems [8]. We then extend these results to more complicated situations with $N = 3$ and $N = 4$, noting that many of these results are valid for larger values of $N$.

## 2. Quantum breathers in a translational invariant lattice

In QDNLS case, we use a number state basis, $|\psi_n\rangle = [n_1, n_2, \ldots, n_f]$, where $n_i$ represents the number of quanta at site $i$ ($N = \sum_n n_i$). A general wave function is $|\Psi_n\rangle = \sum_n a_n |\psi_n\rangle$. For example, in the case $f = 2$ and $N = 2$, the most general eigenfunction of the boson number operator is $|\Psi_n\rangle = a_1[2, 0] + a_2[0, 2] + a_3[1, 1]$. Occasionally for plotting purposes we use a basis that emphasises the positions of the two bosons along the chain, $n_1$ and $n_2$. In this case our example wave function becomes $|\Psi_n\rangle = c_{1,1}[2, 0] + c_{2,2}[0, 2] + \frac{1}{\sqrt{2}}(c_{1,2} + c_{2,1})[1, 1]$, where $c_{1,2}$ indicates that the first boson is located at $n_1 = 1$ and the second one in $n_2 = 2$. As bosons are indistinguishable quanta, $c_{i,j} = c_{j,i}$.

In homogeneous quantum lattices with periodic boundary conditions, it is possible to block-diagonalize the Hamiltonian operator using eigenfunctions of the translation operator with fixed value of the momentum $k$ [2].

As shown in Fig. 1, if the anharmonicity parameter is high enough, there exists an isolated ground state eigenvalue for each $k$ which corresponds to a quantum breather. By this we mean there is a high probability of finding the quanta on the same site, but due to the translational invariance of the system, an equal probability of finding these quanta at any site of the system. In these cases, some analytical expressions can be obtained in some asymptotic limits (studies of this problem go back to the 30s, for recent discussions see [2,7, 9]).

In particular, in the case $N = 2$ and working at $k = 0$ for simplicity, the ground state unnormalized eigenfunction is

$$|\Psi\rangle = [20\ldots0] + [020\ldots0] + \cdots + [0\ldots02] + O(\gamma^{-1}),$$

i.e., on a lattice of length $f$, the unnormalized coefficients $a_i$ of the first $f$ terms are equal to unity and the rest are $O(\gamma^{-1})$. In the extreme of complete spatial localization, one of these $a_i$ would be unity and the rest zero.
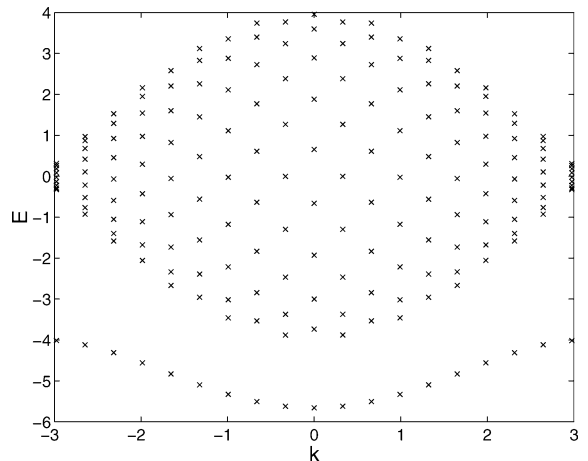


Fig. 1. Eigenvalues $E(k)$. $N = 2$, $f = 19$ and $\gamma = 4$.

## 3. Trapping in a lattice with broken translational symmetry

In this section we study how the components $a_i$ change as the translational invariance of the lattice is broken in various ways. In these cases, the Hamiltonian operator cannot be block-diagonalized using eigenvectors of the translation operator. Although the computational effort increases, it is still possible to calculate eigenvalues and eigenvectors if $f$ and $N$ are small enough, by using algebraic manipulation methods to construct an exact Hamiltonian matrix in algebraic form and then a numerical eigenvalue solver. In this section we restrict ourselves to the simplest nontrivial case $N = 2$.

One simple way to break translational invariance is to consider a finite chain with no-flux boundary conditions. In this case, the solution becomes weakly localized around the middle of the lattice. If $f$ is high enough, and we ignore boundary effects, this case reduces to the homogeneous lattice case.

An alternative mechanism to break translational invariance is the existence of local inhomogeneities or impurities that can affect the nonlinear localized modes considerably. In systems with both nonlinearity and impurities, it is important to understand the interplay between these two sources of localization. For these cases we break translational invariance by making one or more of the $\gamma_j$ or the $\epsilon_j$ depend on $j$. This may occur because of localized impurities, or because the chain geometry becomes nonuniform. Two examples of nonuniform geometries are shown in Fig. 2.

Fig. 2(a) shows a circular chain twisted into a figure-of-eight, so that two sites on the chain, well separated along the length of the chain, become spatially close. This toy model for a globular protein was studied in [10], where it was shown that moving breathers described by the classical DNLS equation could become trapped at the cross-over point. In the quantum case such a geometry can be modelled by adding a term such as

$$\alpha_{\ell,m}\big(b_\ell^\dagger b_m + b_m^\dagger b_\ell\big), \tag{2}$$

to the Hamiltonian, where $\ell$ and $m$ are the two sites brought close together by the twist, and $\alpha_{\ell,m}$ is the separation distance relative to the unit length of the unperturbed chain. This can be considered as a special case of a chain with long-range coupling. See also [11] for a more realistic protein simulation, and [12] for other discussions on the effects of chain geometry on moving breathers.

The bent chain in Fig. 2(b) shows another possible geometry which has been studied recently in the classical DNLS case. In this case we have an abrupt bend which is simulated by adding an additional term as in (2) but where $m = m_0 - 1$, $\ell = m_0 + 1$, where $m_0$ is the vertex of the bend. By varying the values of $\alpha_{\ell,m} = \alpha$, all angles between 0 and $\pi$ can be simulated approximately. The influence of this geometry has been analyzed in the DNLS context in [13], and in nonlinear Klein–Gordon systems in [14]. This geometry is of interest in nonlinear photonic crystals waveguides and circuits [15].

Localization due to random variation of the lattice parameters has long been studied in the harmonic model since the pioneering work of Anderson [16]. Our interest is to see what new localization effects the anharmonic terms bring to the model, and to what extent the anharmonic effects enhance the Anderson-like localization effect when this is present in the harmonic model ($\gamma_i = 0$). See also the discussions in [17].

Most of our findings are not specific to the QDNLS model, for example, we have repeated our calculations using the attractive fermionic Hubbard model with two particles of opposite spins [18]. Although all the models we consider have a conserved number, in general they are not quantum integrable.

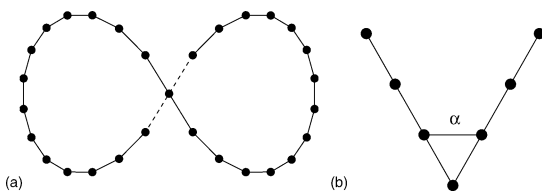We now consider the effects introduced above in more detail.



Fig. 2. Two nonuniform chain geometries.

## 4. Localization in a straight chain with impurities

In this version of our model, in order to explore the interplay between the localization induced by the nonlinearity and the influence of a impurity in these localized states, we introduce a local inhomogeneity
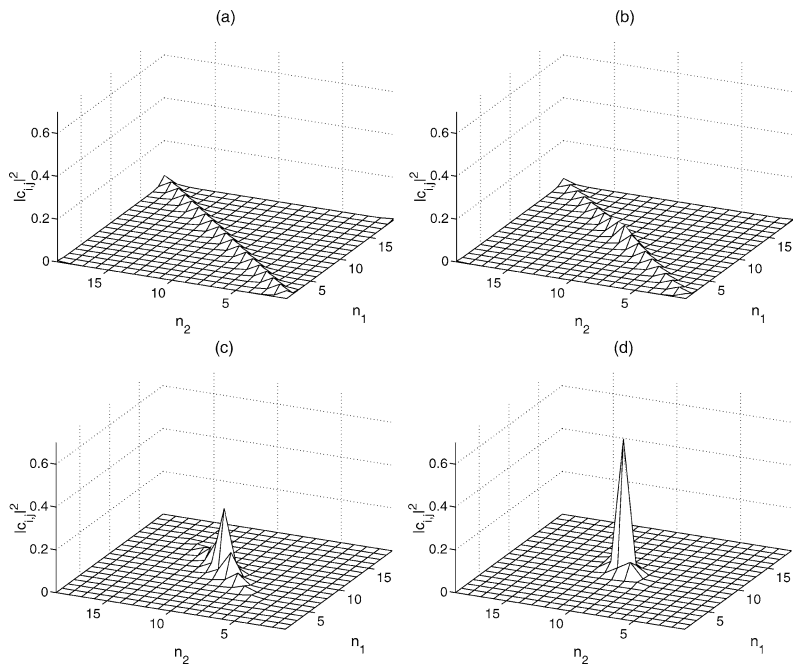
Fig. 3. Square wave function amplitudes $|c_{i,j}|^2$ corresponding to the ground state as a function of the positions $n_1$, $n_2$ of the two bosons on the chain. We have $f = 19$ and $\gamma = 4$ and a point impurity at $\ell = 10$. (a) Homogeneous chain, (b) $\gamma_{\text{im}} = 4.1$, (c) $\gamma_{\text{im}} = 4.4$, (d) $\gamma_{\text{im}} = 5$.

in the anharmonic parameter. To isolate the effect of the impurity of other effects related to the finite size of the chain, we retain the periodic boundary conditions. The anharmonicity parameter is $\gamma_\ell = \gamma_{\text{im}}$, and $\gamma_j = \gamma$ for $j \neq \ell$.

In the homogeneous system ($\gamma_{\text{im}} = \gamma$), with $\gamma$ large enough, as discussed above, the ground state is "localized" in the sense that there exist a high probability to find the two quanta on the same site, but with equal probability at any site of the chain. For the chain with a point impurity, we plot in Fig. 3 the coefficients of the components of the ground state wave function for various values of $\gamma_{\text{im}}$. As $\gamma_{\text{im}}$ increases, these coefficients start from an initial spatially uniform distribution, but then localize around the site of the impurity, in this case at $\ell = 10$. At the largest value of $\gamma_{\text{im}}$ shown, over 60% of the wave function is in the state $[0\ldots 020\ldots 0]$, with the two bosons at site 10. Also, there exists some localization corresponding to the coefficients of states where the two bosons are on neighbouring sites, and one of them at the impurity, but this effect is much weaker for these components. Other components are even smaller.
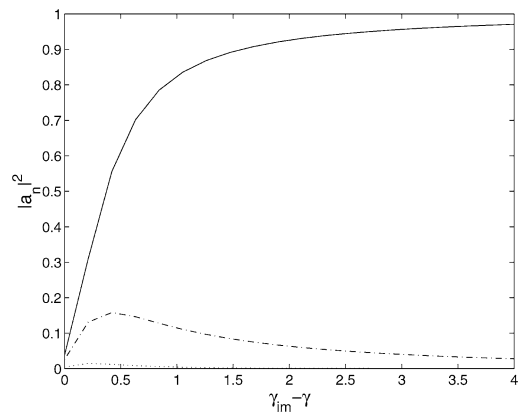


Fig. 4. Some components of the wave function corresponding to the ground state. $N = 2$, $f = 19$ and $\gamma = 4$. Curves correspond to (—) two bosons centered on the impurity, $(- \cdot -)$ two bosons in adjacent sites with one of them centered on the impurity, $(\cdots)$ two bosons separated by one site and one of them at the impurity.

In Fig. 4, we plot the size of components of the wave function of the ground state corresponding to the two bosons centered at the local inhomogeneity at the same site, at adjacent sites, and separated by one site. We observe that the localization increases very rapidly

with the magnitude of the impurity. Note that there is no Anderson-like effect in this case as the harmonic terms are homogeneous.

## 5. The twisted chain

For the twisted chain as shown in Fig. 2(a), the only extra parameter is $\alpha_{m,\ell}$, the strength of the long range coupling between the two spatially adjacent sites $m$ and $\ell$. As an example we consider the case $\alpha_{m,\ell} = 1$, $f = 19$, $m = 5$, and $\ell = 15$. Fig. 5 shows the components of the ground state wave function, plotted as a function of $\gamma$.

A breather localized at the crossover point $m = 5$, $\ell = 15$, will show an enhanced coefficient corresponding to localization at the two points of the chain which come together. With $\gamma = 0$, we see some small localization effect at sites $m$ and $\ell$ for the $[0\ldots020\ldots0]$ coefficients at the crossover points, corresponding to a harmonic Anderson-like effect. However, for nonzero $\gamma$ we see that this effect is strongly enhanced. The coefficient of the components corresponding to the two

bosons in contiguous sites show a weaker localization as before. Similar results are obtained for other values of $\alpha_{m,\ell}$, with the strength of the localization depending on the size of $\alpha_{m,\ell}$. These trapped quantum states mirror the trapping of the classical mobile breather studied in [10].

## 6. The bent chain

For the bent QDNLS chain (Fig. 2(b)), we follow the classical DNLS treatment [13]. We consider the Hamiltonian (1) on a finite lattice with the additional term (2). The parameter $\alpha$ is related to the wedge angle $\theta$ through $\alpha = \frac{1}{2}(1 - \cos\theta)^{-1}$, and we take the site of the vertex to be $m_0 = \frac{1}{2}(f + 1)$.

Fig. 6 shows the components of the wave function for various values of $\theta$. Fig. 7 shows some components of the ground state wave function corresponding to the neighbors of the vertex, for both $\gamma = 0$ and $\gamma = 4$. If the angle $\theta$ is close to $\pi$, the behavior is similar to the straight chain. The ground state is weakly localized around the center (vertex) of the
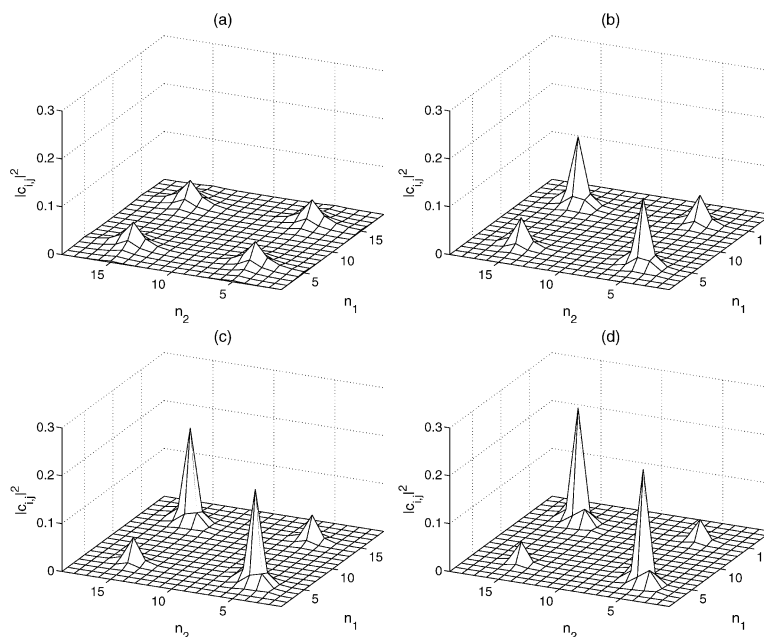


Fig. 5. Square wave function amplitudes $|c_{i,j}|^2$ corresponding to the ground state as a function of the positions $n_1, n_2$ of the two bosons along the twisted chain. Long range interaction between sites $m = 5$ and $\ell = 15$ with $\alpha_{m\ell} = 1$ and $f = 19$. (a) $\gamma = 0$ (harmonic case); (b) $\gamma = 2$; (c) $\gamma = 3$; (d) $\gamma = 4$.
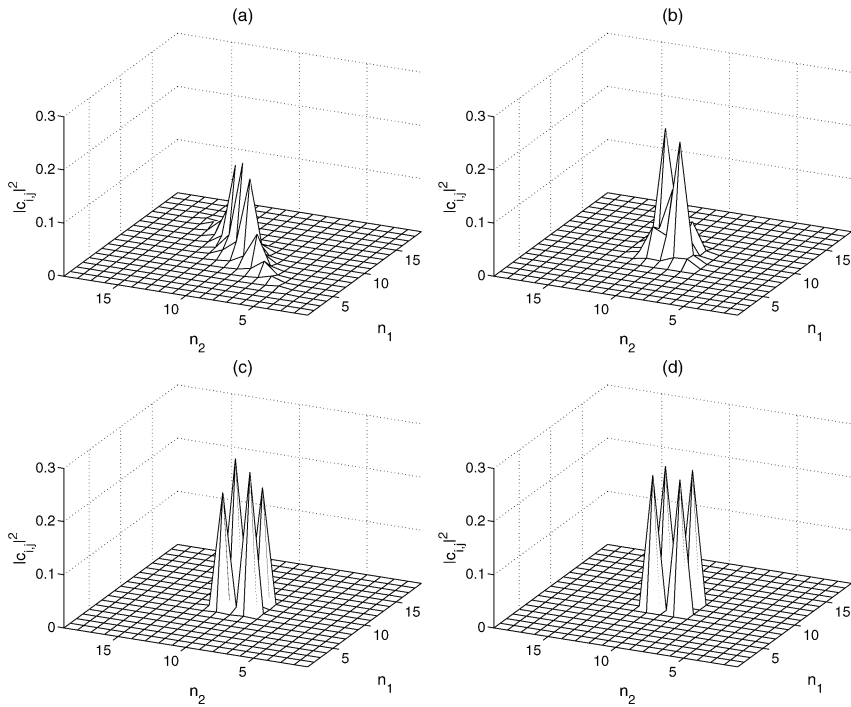
Fig. 6. Square wave function amplitudes $|c_{i,j}|^2$ corresponding to the ground state as a function of the positions $n_1, n_2$ of the two bosons. $f = 19$ and $\gamma = 4$. (a) $\theta = \pi$; (b) $\theta = \pi/3$; (c) $\theta = \pi/10$; (d) $\theta = \pi/100$.
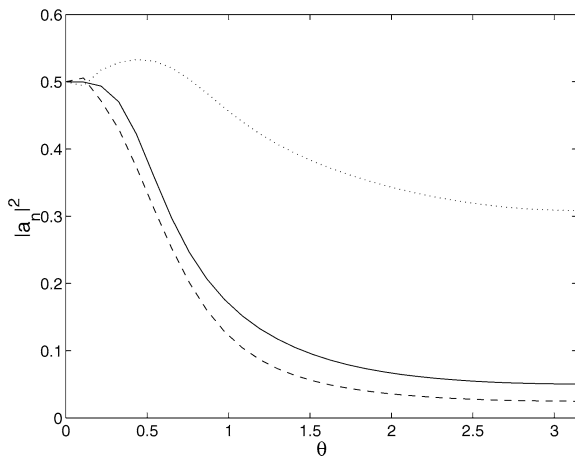


Fig. 7. Some components of the wave function corresponding to the ground state. $N = 2$, $f = 19$. (—) two bosons in a nonlocalized state at neighbouring sites of the vertex and $\gamma = 0$, ($\cdots$) two bosons in a localized state at neighbouring sites of the vertex and $\gamma = 4$, (- - -) two bosons in a nonlocalized state at neighbouring sites of the vertex and $\gamma = 4$.

chain. As $\theta$ decreases, the localization around the vertex increases, and when this angle is small enough, the largest components of the wave function in the ground state consists of states localized around the vertex and the two connected neighboring sites. In the limit $\theta \to 0$, the lattice becomes a T-junction, a model of interest in its own right. It is interesting that the localization in the anharmonic model exhibits a maximum at $\theta \approx 0.5$, whereas in the harmonic case the maximum is at $\theta = 0$. Also the anharmonic enhancement goes to zero as $\theta \to 0$.

We consider here only a long-range interaction between the two vertices of the chain. More realistic models with long-range interaction between all neighbours in the chain give qualitatively the same localization phenomena: a full description will be given elsewhere.

## 7. Higher number of quanta

In previous sections, we restricted our studies to the case $N = 2$. Proceeding as the same way, it is
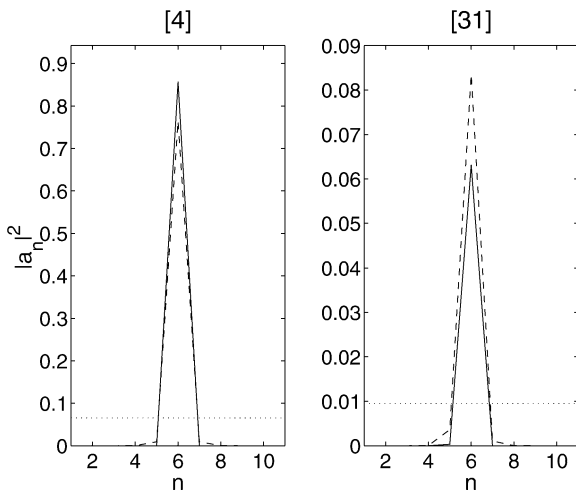
Fig. 8. Square wave function amplitudes $|a_n|^2$ corresponding to some components of the ground state. $f = 11$, $N = 4$ and $\gamma = 2$. Point impurity at the site $\ell = 6$. $(\cdots)$ homogeneous chain case, $\gamma_{im} = 2$, $(\text{- - -})$ $\gamma_{im} = 2.1$, $(\text{---})$ $\gamma_{im} = 2.5$.

possible—in principle—to construct the Hamiltonian matrix for any value of the quantum number $N$ and to calculate the spectrum. However, the computational effort increases rapidly and can go beyond the limits of computational convenience. Nevertheless, we have studied some cases involving a higher number of bosons. In particular, the cases $N = 3$ and $N = 4$.

In general, we have found the same qualitative behavior as in the previous case. In the homogeneous system, if the anharmonic parameter is high enough, the ground state is mainly a bound state, in the sense that there exists a high probability to find all the bosons at the same point of the lattice, but due to the translational invariance of the system, with equal probability of finding these quanta at any site of the chain. When we introduce some local inhomogeneities in the system, we have observed similar localization phenomena as noted above. This effect is stronger when the number of bosons increases.

In Fig. 8 we plot the coefficients of some of the components of the ground state wave function for the case $N = 4$ with a point impurity for various values of $\gamma_{im}$. The left-hand figure shows the coefficients of the $[40\ldots]$, $[040\ldots]$, ... components. As $\gamma_{im}$ increases, these coefficients start from an initial spatially uniform distribution, but then localize around the site of the impurity, in this case at $\ell = 6$. The right-hand figure shows the corresponding coefficients of the $[310\ldots]$, $[0310\ldots]$, ... components. Again some localization is found as $\gamma_{im}$ increases, but this effect is much weaker for these components. Other components (not shown) are even smaller.

## 8. Conclusions

We have shown some results related to the existence and properties of quantum breathers in a system of bosons described by the quantum discrete nonlinear Schrödinger equation. Spatial localizion occurs due to the nonlinearity and to the influence of local inhomogeneities. In particular, we have found that these local inhomogeneities, due to geometrical factors and to long-range interactions or impurities in the anharmonicity parameter, break the translational invariance of the system and localize the ground state around a particular site of the chain. We expect that these results could be extended to a variety of systems.

## Acknowledgements

## References

[1] S. Flach, C.R. Willis, Phys. Rep. 295 (1998) 181;
S. Flach, R.S. MacKay (Eds.), Physica D 119 (1999), special volume;
P.G. Kevrekidis, K.Ø. Rasmussen, A.R. Bishop, Int. J. Mod. Phys. B 15 (2001) 2833;
Yu.S. Kivshar, S. Flach (Eds.), Chaos 13 (2003) 586, focus issue;
L. Vázquez, R.S. MacKay, M.P. Zorzano (Eds.), Localization and Energy Transfer in Nonlinear Systems, World Scientific, Singapore, 2003.

[2] A.C. Scott, J.C. Eilbeck, H. Gilhøj, Physica D 78 (1994) 194;
J. Dorignac, J.C. Eilbeck, M. Salerno, A.C. Scott, Phys. Rev. Lett. 93 (2004) 025504.

[3] V. Fleurov, Chaos 13 (2003) 676;
R.S. MacKay, Physica A 288 (2000) 174.

[4] F. Fillaux, C.J. Carlile, G.J. Kearley, Phys. Rev. B 58 (1998) 11416;

B.I. Swanson, et al., Phys. Rev. Lett. 82 (1999) 3288;
T. Asano, et al., Phys. Rev. Lett. 84 (2000) 5880;
L.S. Schulman, et al., Phys. Rev. Lett. 88 (2002) 224101.

[5] X. Li, et al., Science 301 (2003) 809.

[6] G.L. Alfimov, V.V. Konotop, M. Salerno, Europhys. Lett. 58 (2002) 7;
R. Carretero-González, K. Promislow, Phys. Rev. A 66 (2002) 033610.

[7] A.C. Scott, Nonlinear Science, Oxford Univ. Press, Oxford, 1999.

[8] P. Jakob, Appl. Phys. A: Mater. Sci. Proc. 75 (2002) 45.

[9] J.C. Eilbeck, in: L. Vazquez, R.S. MacKay, M.P. Zorzano (Eds.), Localization and Energy Transfer in Nonlinear Systems, World Scientific, Singapore, 2003, p. 177.

[10] J.C. Eilbeck, in: C. Kawabata, A.R. Bishop (Eds.), Computer Analysis for Life Science, Ohmsha, Tokyo, 1986, p. 12.

[11] H. Feddersen, Phys. Lett. A 154 (1991) 391.

[12] P.G. Kevrekidis, B.A. Malomed, A.R. Bishop, Phys. Rev. E 66 (2002) 046621;
I. Bena, A. Saxena, J.M. Sancho, Phys. Rev. E 66 (2002) 036617;
J. Cuevas, F. Palmero, J.F.R. Archilla, F.R. Romero, Phys. Lett. A 299 (2002) 221.

[13] P.L. Christiansen, Y.B. Gaididei, S.F. Mingaleev, J. Phys.: Condens. Matter 13 (2001) 1181;
Yu.S. Kivshar, P.G. Kevrekidis, S. Takeno, Phys. Lett. A 307 (2003) 287.

[14] J. Cuevas, P.G. Kevrekidis, Phys. Rev. E 69 (2004) 056609.

[15] S.F. Mingaleev, Yu.S. Kivshar, Opt. Photonics News 13 (2002) 48.

[16] P.W. Anderson, Phys. Rev. 109 (1958) 1492.

[17] J.F.R. Archilla, R.S. MacKay, J.L. Marin, Physica D 134 (1999) 406;
G. Kopidakis, S. Aubry, Physica D 139 (1999) 247.

[18] J.C. Eilbeck, F. Palmero, in: F.Kh. Abdullaev, V.V. Konotop (Eds.), Nonlinear Waves: Classical and Quantum Aspects, Kluwer, Amsterdam, 2004, p. 399.